







Search for a Black Hole Binary in Gaia DR3 Astrometric Binary Stars with Spectroscopic Data

ATARU TANIKAWA ¹, KOHEI HATTORI ^{2,3}, NORITA KAWANAKA ⁴, TOMOYA KINUGAWA ⁵, MINORI SHIKAUCHI ^{6,7,8}
AND DAICHI TSUNA ⁷

¹*Department of Earth Science and Astronomy, College of Arts and Sciences, The University of Tokyo, 3-8-1 Komaba, Meguro-ku, Tokyo 153-8902, Japan*

²*National Astronomical Observatory of Japan, 2-21-1 Osawa, Mitaka, Tokyo 181-8588, Japan*

³*Institute of Statistical Mathematics, 10-3 Midoricho, Tachikawa, Tokyo 190-8562, Japan*

⁴*Center for Gravitational Physics and Quantum Information, Yukawa Institute for Theoretical Physics, Kyoto University, Kitashirakawa Oiwake-cho, Sakyo-ku, Kyoto 606-8502, Japan*

⁵*Institute for Cosmic Ray Research, University of Tokyo, Kashiwa, Chiba 255-8582, Japan*

⁶*Department of Physics, the University of Tokyo, 7-3-1 Hongo, Bunkyo, Tokyo 113-0033, Japan*

⁷*Research Center for the Early Universe (RESCEU), School of Science, The University of Tokyo, 7-3-1 Hongo, Bunkyo-ku, Tokyo 113-0033, Japan*

⁸*Department of Physics and Astronomy, the University of British Columbia, 6224 Agricultural Road, Vancouver, BC, V6T 1Z1, Canada*

ABSTRACT

We report the discovery of a candidate binary system consisting of a black hole (BH) and a red giant branch star from the Gaia DR3. This binary system is discovered from 64108 binary solutions for which both astrometric and spectroscopic data are available. For this system, the astrometric and spectroscopic solutions are consistent with each other, making this system a confident candidate of a BH binary. The primary (visible) star in this system, Gaia DR3 5870569352746779008, is a red giant branch whose mass is quite uncertain. Fortunately, albeit the uncertainty of the primary’s mass, we can estimate the mass of the secondary (dark) object in this system to be $> 5.68 M_{\odot}$ with a probability of 99 %, based on the orbital parameters. The mass of the secondary object is much larger than the maximum neutron star mass ($\sim 2.0 M_{\odot}$), which indicates that the secondary object is likely a BH. We argue that, if this dark object is not a BH, this system must be a more exotic system, in which the primary red giant branch star orbits around a quadruple star system (or a higher-order multiple star system) whose total mass is more than $5.68 M_{\odot}$. If this is a genuine BH binary, this has the longest period (1352.22 ± 45.81 days) among discovered so far. As our conclusion entirely relies on the Gaia DR3 data, independent confirmation with follow-up observations (e.g. long-term spectra) is desired.

Keywords: Stellar mass black holes – Astrometric binary stars – Spectroscopic binary stars

1. INTRODUCTION

Stellar-mass black holes (BHs) are the final state of massive stars with several $10 M_{\odot}$ (e.g. Woosley et al. 2002). BHs are not just dark, especially when they are members of close binary stars. Thus, they have been discovered as X-ray binaries (e.g. Casares et al. 2017) and gravitational wave transients (Abbott et al. 2019, 2021; The LIGO Scientific Collaboration et al. 2021). Nevertheless, since such BH populations are rare, just a

handful of BHs are known. So far, ~ 100 BHs have been detected as X-ray binaries in the Milky Way, (Corral-Santana et al. 2016), while there should be $\sim 10^8$ BHs in the Milky Way (e.g. Shapiro & Teukolsky 1983; van den Heuvel et al. 1992). This is because BHs are bright in X-rays only when they have close companion stars: binary periods of less than about 1 day.

Great efforts have been made to discover a variety of BHs in binary stars (hereafter BH binaries). Many spectroscopic observations have reported BH binaries with periods of 1–100 days (Thompson et al. 2019; Liu et al. 2019; Rivinius et al. 2020; Jayasinghe et al. 2021, 2022b; Lennon et al. 2022; Saracino et al. 2022). However, many concerns have been raised for these reports

(Abdul-Masih et al. 2020; El-Badry & Quataert 2020; van den Heuvel & Tauris 2020; El-Badry & Quataert 2021; Eldridge et al. 2020; Irrgang et al. 2020; Tanikawa et al. 2020; Safarzadeh et al. 2020; Bodensteiner et al. 2020; Shenar et al. 2020; El-Badry & Burdge 2022; El-Badry et al. 2022a,b). Several BH binaries (Giesers et al. 2018; Shenar et al. 2022) still survive, despite such harsh environment for BH binary searchers.

Gaia have monitored more than 10^9 stars and their astrometric and spectroscopic motions during 34 months (Gaia Collaboration et al. 2016, 2018a, 2021, 2022a), and have published $\sim 3 \times 10^5$ astrometric and spectroscopic binary stars in total in Gaia Data Release 3 (GDR3; Gaia Collaboration et al. 2022b; Holl et al. 2022a,b; Halbwachs et al. 2022). Before GDR3, many studies have predicted that *Gaia* discovers a large amount of compact objects in binary stars, such as white dwarfs (WDs), neutron stars (NSs), and BHs, from *Gaia*’s astrometric data (Mashian & Loeb 2017; Breivik et al. 2017; Yalinewich et al. 2018; Yamaguchi et al. 2018; Kingawa & Yamaguchi 2018; Shahaf et al. 2019; Shao & Li 2019; Andrews et al. 2019, 2021; Shikauchi et al. 2020, 2022; Chawla et al. 2022; Janssens et al. 2022). Starting with Gaia Collaboration et al. (2022b), many research groups have searched for WD, NS, and BH binaries in spectroscopic binaries (Gomel et al. 2022; Jayasinghe et al. 2022a; Fu et al. 2022) and astrometric binaries (Andrews et al. 2022; Chakrabarti et al. 2022; El-Badry et al. 2023a; Shahaf et al. 2023) just after GDR3.

GDR3 has presented several 10^4 binary stars with both of astrometric and spectroscopic data. However, previous studies have focused on either of astrometric or spectroscopic data. In this paper, we first search for BH binaries from binary stars where both data are available, taking into account both of astrometric and spectroscopic data. In other words, we first make a comparison between astrometric and spectroscopic mass functions (see Eqs. (1) and (3), respectively) to search for BH binaries.

We eventually find a promising BH binary candidate whose source ID is GDR3 5870569352746779008. After we posted this work to arXiv, El-Badry et al. (2023a) have independently pointed out that the BH binary candidate is promising, and El-Badry et al. (2023b) have confirmed it as a genuine BH binary by follow-up observations. This shows that our search is helpful and efficient to narrow down BH binary candidates. Although we recognize that El-Badry et al. (2023b) call it “Gaia BH2”, we call it “BH binary candidate” in this paper. This is *not* because we disagree with their confirmation, but because we regarded it as a BH binary candidate when we posted this work to arXiv (September 2022).

The structure of this paper is as follows. In section 2, we describe how to select a sample of binary stars from GDR3, and how to list up BH binary candidates. Finally, we find one BH binary candidate. In section 3, we analyze the BH binary candidate in detail. In section 4, we discuss the BH binary candidate, comparing it with BH binary candidates listed by previous studies. In section 5, we summarize this paper.

2. SAMPLE SELECTION

2.1. Search for BH binaries with $m_2 > 3M_\odot$

We select GDR3 binary stars with astrometric and spectroscopic data (Gaia Collaboration et al. 2022b). There are three types of such binary stars. The orbital solutions of the first type are obtained from astrometric and spectroscopic data. They have a `nss_solution_type` name of “AstroSpectroSB1” in the non-single star tables of GDR3 (`nss_two_body_orbit`). We call them AstroSpectroSB1 binary stars. The second type has an orbital solution derived only from astrometric data, and additionally has the total amplitude in the radial velocity time series called “rv_amplitude_robust”. Such binary stars have a `nss_solution_type` name of “Orbital”, and satisfy the following two conditions. First, they are bright stars; they have *Gaia* RVS magnitude less than and equal to 12. Second, their radial velocities are computed more than twice. For the third type, binary stars have two `nss_solution_type` names of “Orbital” and “SB1” independently. Such binary stars also have a `non_single_star` value of 3. Hereafter, the second and third types are collectively called Orbital binary stars simply. We can extract such a sample of binary stars from GDR3 with following ADQL query:

```
select nss.*, gs.*
from gaiadr3.nss_two_body_orbit as nss,
gaiadr3.gaia_source as gs
where nss.source_id = gs.source_id
and (nss.nss_solution_type = 'AstroSpectroSB1'
     or (nss.nss_solution_type = 'Orbital'
         and gs.rv_amplitude_robust IS NOT NULL)
     or gs.non_single_star = 3)
```

The line numbers 5, 6-7, and 8 in the above ADQL query try to pick up the first, second and third types, respectively. However, the line number 8 picks up binary stars not only the third type binaries but also many other binaries, for example, binary stars with `nss_solution_type` names of “acceleration7” and “SB1”. We exclude them later. Finally, the total number of binary stars is 64108 consisting of 33467 “AstroSpectroSB1” and 30641 “Orbital” binary stars, where the

numbers of the second and third types are 30629 and 12, respectively.

We search for BH binary candidates from the above sample, using astrometric and spectroscopic mass functions ($f_{\text{m,astro}}$ and $f_{\text{m,spectro}}$, respectively). We express these mass functions as follows:

$$f_{\text{m,astro}} = (m_1 + m_2) \left| \frac{m_2}{m_1 + m_2} - \frac{F_2/F_1}{1 + F_2/F_1} \right|^3 \quad (1)$$

$$= 1 \left(\frac{a_1}{\text{mas}} \right)^3 \left(\frac{\varpi}{\text{mas}} \right)^{-3} \left(\frac{P}{\text{yr}} \right)^{-2} [M_\odot], \quad (2)$$

and

$$f_{\text{m,spectro}} = (m_1 + m_2) \left(\frac{m_2}{m_1 + m_2} \right)^3 \quad (3)$$

$$= 3.7931 \times 10^{-5} \left(\frac{K_1}{\text{km s}^{-1}} \right)^3 \left(\frac{P}{\text{yr}} \right) \times (1 - e^2)^{3/2} \sin^{-3} i [M_\odot], \quad (4)$$

where m_1 and m_2 are the primary and secondary stars of a binary star, F_2/F_1 is the flux ratio of the secondary star to the primary star, a_1 is the angular semi-major axis of the primary star, K_1 is the semi-amplitude of the radial velocity of the primary star, and ϖ , P , e , and i are the parallax, period, eccentricity, and inclination angle of the binary star, respectively. We define a primary star as a star observed by astrometry and spectroscopy, and a secondary star as a fainter star than the primary star. The secondary star is an unseen star if $F_2/F_1 = 0$. We can get a_1 , ϖ , P , e , and i from astrometry, and K_1 from spectroscopy. We have to remark that $f_{\text{m,spectro}}$ is similar to but different from the spectroscopic mass function ordinarily defined (hereafter $\hat{f}_{\text{m,spectro}}$), since we obtain $f_{\text{m,spectro}}$, dividing $\hat{f}_{\text{m,spectro}}$ by $\sin^3 i$. We can know the inclination angle, i , thanks to astrometric observation, and thus mainly refer to $f_{\text{m,spectro}}$, not $\hat{f}_{\text{m,spectro}}$.

Practically, we calculate $f_{\text{m,spectro}}$ of **AstroSpectroSB1** binary stars as

$$f_{\text{m,spectro}} = \left[\left(\frac{C_1}{\text{au}} \right)^2 + \left(\frac{H_1}{\text{au}} \right)^2 \right]^{3/2} \left(\frac{P}{\text{yr}} \right)^{-2} \sin^{-3} i [M_\odot], \quad (5)$$

where C_1 and H_1 are Thiele-Innes elements (Bin-nendijk 1960; Heintz 1978), derived by spectroscopic observation. On the other hand, we calculate $f_{\text{m,spectro}}$ of **Orbital** binary stars, substituting half `rv_amplitude_robust` into K_1 .

We regard binary stars as BH binary candidates if they satisfy the following two conditions:

$$0.5 \leq f_{\text{m,spectro}}/f_{\text{m,astro}} \leq 2, \quad (6)$$

$$f_{\text{m,astro}} \geq 3M_\odot. \quad (7)$$

We adopt the first condition expressed by Eq. (6) for the following reason. When a binary star is a BH binary, the secondary star is an unseen star; $F_2/F_1 = 0$. Substituting $F_2/F_1 = 0$ into Eq. (1), we find $f_{\text{m,astro}} = f_{\text{m,spectro}}$. Thus, BH binaries should satisfy $f_{\text{m,astro}} \simeq f_{\text{m,spectro}}$. By the second condition of Eq. (7), we can select binary star candidates with $m_2 \geq 3M_\odot$ irrespective of m_1 . Such binary stars are likely to be BH binaries, since the maximum mass of neutron stars is expected to be $\sim 2M_\odot$ (Kalogera & Baym 1996).

Figure 1 shows $f_{\text{m,astro}}$ and $f_{\text{m,spectro}}/f_{\text{m,astro}}$ of all the samples. The shaded region in this figure corresponds to the two conditions imposed in this study (Eqs. (6) and (7)). Only one binary star satisfies these two conditions. Its basic parameters are summarized in Table 1. We analyze this BH binary candidate in later sections.

In general, we have $f_{\text{m,spectro}} \geq f_{\text{m,astro}}$ for any binary stars, which can be easily confirmed from their definitions in Eq. (1) and Eq. (3). However, Figure 1 shows that the distribution of $f_{\text{m,spectro}}/f_{\text{m,astro}}$ spreads under 1. There can be two reasons. First, $f_{\text{m,spectro}}$ is underestimated for the second type of binary stars. For these binary stars, we adopt `rv_amplitude_robust` for K_1 in Eq. (4). However, the observed radial velocities may not fall at the right phase to fully sample the orbit's maximum and minimum radial velocities. Second, some of binary stars contain large errors of either $f_{\text{m,spectro}}$ or $f_{\text{m,astro}}$, while they have $f_{\text{m,spectro}} \geq f_{\text{m,astro}}$ in reality. In fact, such binary stars may hide BH binaries. However, in this paper, we conservatively select binary stars with $f_{\text{m,spectro}} \simeq f_{\text{m,astro}}$ as BH binary candidates. This is because the small discrepancy between $f_{\text{m,spectro}}$ and $f_{\text{m,astro}}$ is anticipated for a binary system in which the secondary star is much fainter than the primary star ($F_2/F_1 \simeq 0$).

It is a bit strange that the $\log(f_{\text{m,spectro}}/f_{\text{m,astro}})$ values are centered on zero for both the **AstroSpectroSB1** and **Orbital** binary stars. Typically, binary stars should have luminous secondary stars (e.g. Sana et al. 2012), and thus should have F_2/F_1 close to 1, and large $f_{\text{m,spectro}}/f_{\text{m,astro}}$ (or small $f_{\text{m,astro}}$). The reason for this discrepancy might be that *Gaia* preferentially select binary stars with faint secondary stars.

Figure 2 shows the distributions of the $\log f_{\text{m,astro}}$ and $\log f_{\text{m,spectro}}$ dispersions for **AstroSpectroSB1** binary stars. In order to obtain these dispersions, we generate 10^3 Monte Carlo random draws of the co-

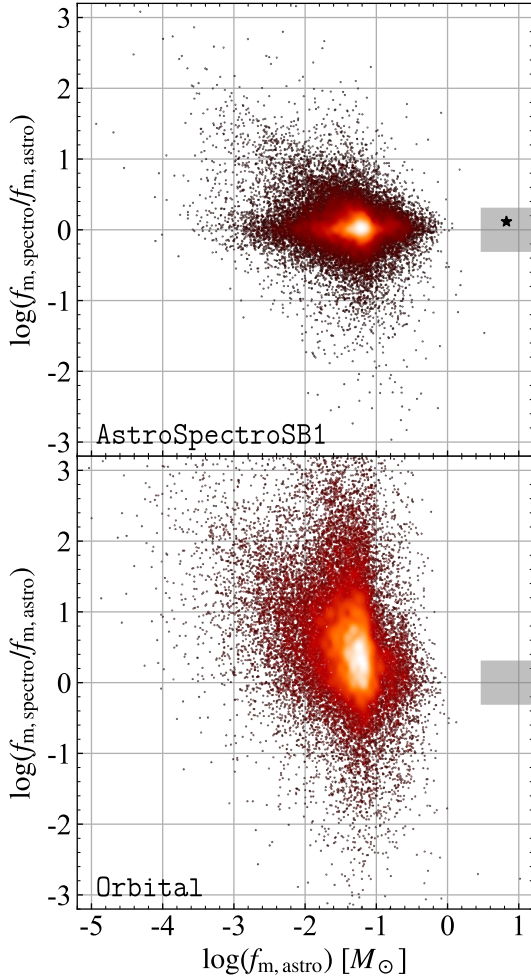


Figure 1. Scatter plots of $f_{m,astro}$ and $f_{m,spectro}/f_{m,astro}$ for **AstroSpectroSB1** (top) and **Orbital** (bottom) binary stars. The color scale represents the square root of the relative density of binary stars. Shaded regions satisfy the two conditions of BH binary candidates expressed as Eqs. (6) and (7). The BH binary candidate found in this work (GDR3 5870569352746779008) is emphasized as a star in the top panel.

variance matrix of the BH binary candidate in the GDR3 `nss_two_body_orbit` table. Note that the number of Monte Carlo random draws is sufficient, since the distributions for 10^3 random draws are similar to those for 10^2 random draws. We cannot calculate the $\log f_{m,spectro}$ dispersions of **Orbital** binary stars, since the covariance matrix does not include the data of `rv_amplitude_robust`. The $\log f_{m,spectro}$ dispersions of **Orbital** binary stars should be larger than that of **AstroSpectroSB1** binary stars. This is also the reason why $\log(f_{m,spectro}/f_{m,astro})$ values spread more widely in **Orbital** binary stars than in **AstroSpectroSB1** binary stars. The peak of the $\log f_{m,spectro}$ dispersion is

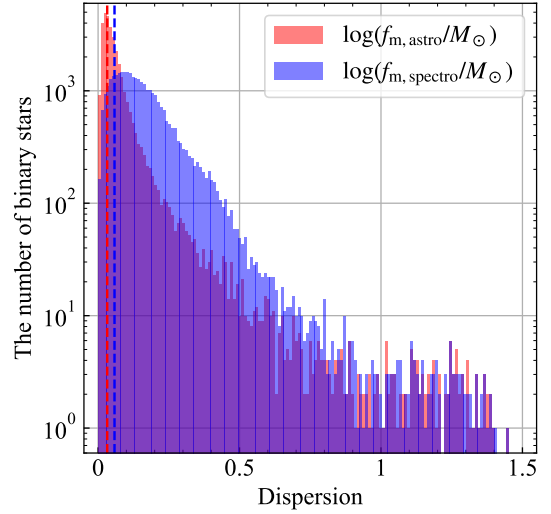


Figure 2. Distributions of the $\log f_{m,astro}$ and $\log f_{m,spectro}$ dispersions for **AstroSpectroSB1** binary stars. The red and blue dashed lines indicate the $\log f_{m,astro}$ and $\log f_{m,spectro}$ dispersions, respectively, for the BH binary candidate (GDR3 source ID 5870569352746779008).

at ~ 0.2 . On the other hand, $\gtrsim 100$ binary stars have the $\log f_{m,spectro}$ dispersions of $\gtrsim 1$. This should affect the presence of binary stars with $\log f_{m,spectro}/f_{m,astro} < 0$.

If a binary star system is actually a triple star system, $f_{m,spectro}$ will be significantly overestimated, and consequently $f_{m,spectro} > f_{m,astro}$ for the following reason. Astrometric observation is sensitive to the outer binary's motion: the relative motion between the inner binary and third star. On the other hand, spectroscopic observation is sensitive to the inner binary's motion, since its motion velocity is much larger than the outer binary's motion velocity. Thus, we will calculate $f_{m,spectro}$ in Eq. (4), using P , e , and i of the outer binary and K_1 of the inner binary. This $f_{m,spectro}$ will be larger than the actual $f_{m,spectro}$ of both the inner and outer binaries. For obtaining the inner (outer) binary's $f_{m,spectro}$, the adopted P (K_1) is larger than the actual inner (outer) binary's. This may happen in the **Orbital** binary stars more frequently.

2.2. Some comments on rejected binaries

Before analyzing the BH binary candidate in detail, we review our search. In particular, we focus on binary stars which look like BH binaries at a glance, but which our search rejects. GDR3 provides the `binary_masses` table including the masses of primary and secondary stars estimated from the PARSEC isochrone models¹

¹ <http://stev.oapd.inaf.it/cgi-bin/cmd>

(Bressan et al. 2012). We can obtain such binary stars with following ADQL query:

```
select nss.*, gs.*, bm.*
from gaiadr3.nss_two_body_orbit as nss,
gaiadr3.gaia_source as gs,
gaiadr3.binary_masses as bm
where gs.source_id = nss.source_id
and bm.source_id = nss.source_id
and (nss.nss_solution_type = 'AstroSpectroSB1'
or (nss.nss_solution_type = 'Orbital'
and gs.rv_amplitude_robust IS NOT NULL)
or (gs.non_single_star = 3))
```

We just add the `binary_masses` table to the ADQL query in section 2.1. Note that our samples are the ones obtained with the ADQL query in section 2.1 unless otherwise stated. Not all our samples are listed in the `binary_masses` table, because the mass estimation is only applied to primary stars in the main sequence (MS) on the color-magnitude diagram. In the `binary_masses` table, there are 6 `AstroSpectroSB1` and 3 `Orbital` binary stars containing secondary stars with $> 3M_{\odot}$. In spite of their secondary masses, none of them are regarded as BH binary candidates by our search.

As for the 6 `AstroSpectroSB1` binary stars, they are rejected, because all of them have too large $f_{m,\text{spectro}}/f_{m,\text{astro}}$ (> 10). This means that, although these binary stars have main-sequence primary stars with $1\text{--}2 M_{\odot}$, they have secondary stars with $> 3 M_{\odot}$ and smaller (but non-zero) luminosity than the primary stars. It is difficult to interpret these binary stars as BH binaries. Thus, we remove them from our list of BH binary candidates. The 3 `Orbital` binary stars are ruled out, since they have too small $f_{m,\text{spectro}}/f_{m,\text{astro}}$ (< 0.01). Incomprehensibly, their F_2/F_1 values are negative. Astrometric or spectroscopic results might not be appropriate. In fact, all of them have large goodness-of-fit values (> 5), where the goodness-of-fit is expected to obey the normal distribution if astrometric parameters are correctly derived. When Andrews et al. (2022) search for NS and BH binaries, they rule out binary stars with goodness-of-fit values more than 5 from NS and BH binary candidates.

The second condition expressed by Eq. (7) may be too strict to complete a search for BH binaries from our sample. This condition means that the secondary mass is more than $3 M_{\odot}$ for any primary masses. We convert this condition to $m_2 > 3 M_{\odot}$, where m_2 is drawn from the lower limit of m_2 (`m2_lower`) in the GDR3 `binary_masses` table. By this conversion, we can relax our search for BH binaries, since the secondary mass can be more than $3 M_{\odot}$ even for $f_{m,\text{astro}} < 3 M_{\odot}$ if the pri-

mary mass is larger than a certain value. However, we find no other BH binary candidate. Although the two conditions expressed by Eqs. (6) and (7) are slightly strict, we confirm that there is only one BH binary candidate (GDR3 source ID 5870569352746779008) in GDR3 astrometric binary stars with spectroscopic data.

3. ANALYSIS OF A BH CANDIDATE

We summarize the basic parameters of the BH binary candidate in Table 1. For the right ascension, declination, BP-RP color, reddening of BP-RP color, $[M/H]$, and surface gravity ($\log g$), we adopt the mean values in the GDR3 `gaia_source` table. The galactic longitude and latitude are derived from the right ascension and declination. We obtain the mean value of the extinction in G band (A_G) from the EXPLORE G-Tomo scientific data application (Lallement et al. 2022; Vergely et al. 2022)², while the value in the parentheses is the mean value of the GDR3 `gaia_source` table. Hereafter, we adopt the former value for the extinction. We obtain the goodness-of-fit value from the GDR3 `nss_two_body_orbit` table. In order to calculate the mean values and one standard deviation intervals of the distance, period (P), physical semi-major axis (a_1/ϖ), eccentricity (e), inclination (i), radial velocity semi-amplitude (K_1), astrometric mass function ($f_{m,\text{astro}}$), and spectroscopic mass function ($f_{m,\text{spectro}}$), we generate 10^4 Monte Carlo random draws of the covariance matrix of the BH binary candidate in the GDR3 `nss_two_body_orbit` table³. In this method, we also obtain $f_{m,\text{astro}} > 5.68 M_{\odot}$ and $f_{m,\text{spectro}} > 6.57 M_{\odot}$ at a probability of 99 %. Note that the distance is calculated from the parallax in the GDR3 `nss_two_body_orbit` table, not in the GDR3 `gaia_source` table. According to Gaia Collaboration et al. (2022b), the parallax in the former table is more accurate than in the latter table. We get the absolute magnitude in G band (M_G) from the mean of apparent magnitude in the GDR3 `gaia_source`, and the mean of the distance derived above.

The goodness-of-fit value, 3.07, is relatively low, since Andrews et al. (2022) consider that NS and BH binary candidates should have the goodness-of-fit value less than 5. Note that the goodness-of-fit value for reliable sources should be normally distributed with a mean

² <https://explore-platform.eu/>

³ The number of Monte Carlo random draws is sufficiently large, since the results are similar if we adopt 10^3 for the number of the random draws.

Table 1. Basic parameters of the BH binary candidate.

Quantities	Values
(1) Source ID	5870569352746779008
(2) Orbital solution	AstroSpectroSB1
(3) Right ascension	207.5697°
(4) Declination	−59.2390°
(5) Galactic longitude	310.4031°
(6) Galactic latitude	2.7765°
(7) Absolute magnitude in G band (M_G)	1.95 mag
(8) Extinction in G band (A_G)	0.5628 mag (0.70 mag)
(9) BP-RP color	1.49 mag
(10) Reddening of BP-RP color	0.37 mag
(11) Surface gravity ($\log g$, logg_gspphot)	3.25 [cgs]
(12) [M/H] (mh_gspphot)	0.0066 dex
(13) Goodness-of-Fit	3.07
(14) Distance	1164.41 ± 25.16 pc
(15) Period (P)	1352.22 ± 45.81 day
(16) Physical semi-major axis (a_1/ϖ)	4.5194 ± 0.1305 au
(17) Eccentricity (e)	0.5323 ± 0.0153
(18) Inclination (i)	$35.15 \pm 0.99^\circ$
(19) Radial velocity semi-amplitude (K_1)	27.0 ± 1.0 km s ^{−1}
(20) Astrometric mass function ($f_{\text{m,astro}}$)	$6.75 \pm 0.51 M_\odot$
(21) Lower bound in $f_{\text{m,astro}}$ (99%)	$f_{\text{m,astro}} > 5.68 M_\odot$
(22) Spectroscopic mass function ($f_{\text{m,spectro}}$)	$8.85 \pm 1.13 M_\odot$
(23) Lower bound in $f_{\text{m,spectro}}$ (99%)	$f_{\text{m,spectro}} > 6.57 M_\odot$
(24) Probability of $f_{\text{m,spectro}} > f_{\text{m,astro}}$	95 %
(25) Probability of $f_{\text{m,spectro}} < f_{\text{m,astro}}$	5 %

NOTE— From row 3 (right ascension) to 13 (goodness-of-fit) except for row 8 (Extinction in G band), we show the mean value in GDR3. For row 8 (Extinction in G band), the value is obtained from the EXPLORE G-Tomo scientific data application, and the value in the parentheses is obtained from the mean value in GDR3. From row 14 (distance) to 20 ($f_{\text{m,astro}}$) as well as in row 22 ($f_{\text{m,spectro}}$), we show the mean value and one standard deviation interval. In rows 21 and 23, we show the 99% confidence level of $f_{\text{m,astro}}$ and $f_{\text{m,spectro}}$, respectively. In rows 24 and 25, we show the probabilities of $f_{\text{m,spectro}} > f_{\text{m,astro}}$ and $f_{\text{m,spectro}} < f_{\text{m,astro}}$, respectively (see section 3 for more detail).

of zero. Thus, we are not going to arguing that the BH binary candidate is reliable only from the goodness-of-fit value. Nevertheless, we have to remark that the goodness-of-fit value is typical of the **AstroSpectroSB1** binary stars as described later (see Figure 7). Although the goodness-of-fit value largely deviates from zero, it would not directly mean that this BH binary candidate is unreliable. We find that the ratios of means to standard deviation intervals are high for $f_{\text{m,astro}}$ and $f_{\text{m,spectro}}$ (13.2 and 7.83, respectively). They should be relatively well-measured. Additionally, the $\log f_{\text{m,astro}}$

and $\log f_{\text{m,spectro}}$ dispersions are small, compared to those of other **AstroSpectroSB1** binary stars, as seen in Figure 2. This should be another evidence that the parameters of this BH candidate are well-measured. Moreover, at a probability of 99 %, $f_{\text{m,astro}} > 5.68 M_\odot$ and $f_{\text{m,spectro}} > 6.75 M_\odot$. These values are unlikely to fall below $3 M_\odot$. A concern is that $f_{\text{m,spectro}}$ is systematically larger than $f_{\text{m,astro}}$, which we discuss in section 4.

Figure 3 shows the color-magnitude diagram of the primary star of the BH binary candidate, and GDR3

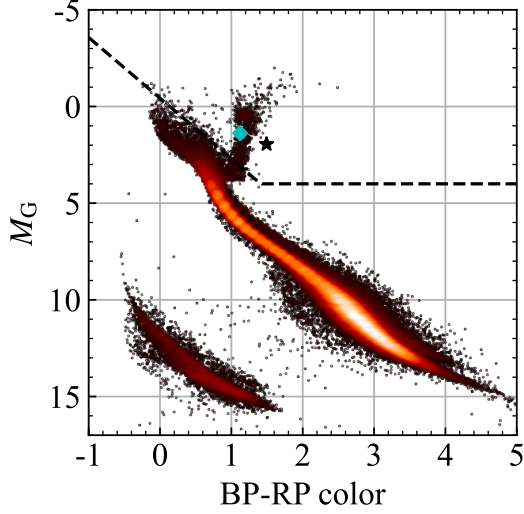


Figure 3. Color magnitude diagram of stars in the GDR3 `gaia_source` table. These stars are filtered in the same way as those in figure 6c of Gaia Collaboration et al. (2018b). The color scale represents the square root of the relative density of stars. The star and diamond points indicate the BH binary candidate (GDR3 source ID 5870569352746779008), where the star and diamond points are not corrected and corrected by its extinction and reddening, respectively. We define the regions of MS and RGB stars below and above the dashed line, respectively. The line is expressed as Eq. (8).

stars whose G-band absolute magnitudes and BP-RP colors are well-measured. MS and red giant branch (RGB) regions are defined as regions below and above the dashed line. The dashed line is expressed as

$$M_G = \begin{cases} 3.14(BP - RP) - 0.43 & (BP - RP < 1.41) \\ 4 & (\text{otherwise}) \end{cases}. \quad (8)$$

The first case of Eq. (8) is the same as in Andrews (2022). We induce the second case to avoid regarding low-mass MS stars as RGB stars. As seen in Figure 3, the primary star of the BH binary candidate is likely to be a RGB star. This is consistent with its small surface gravity ($\log g = 3.25$). The primary star indicated by the star point (not corrected by its extinction and reddening) is redder than RGB stars on the color-magnitude diagram. It suffers from interstellar reddening, since it is located in the Galactic disk ($b = 2.7765^\circ$). In fact, the primary star indicated by the diamond point (corrected by its extinction and reddening) is on the RGB.

Generally, BH binary candidates are thought dubious when their primary stars are RGB stars. This is because such primary stars can easily outshine companion stars even if the companion stars are more massive

than the primary stars. Moreover, it is difficult to estimate the masses of RGB stars in binary systems. Such RGB stars can be in so-called Algol-type systems (El-Badry et al. 2022b). They can be luminous but low-mass (say $\sim 0.1 M_\odot$) if they experience mass transfer. These types of problems frequently happen in BH binary candidates with only spectroscopic data, or usual spectroscopic mass function, $\hat{f}_{m,\text{spectro}}$ (not $f_{m,\text{spectro}}$), and $\hat{f}_{m,\text{spectro}}$ is $\sim 1 M_\odot$. In order to conclude that their secondary stars are $> 3 M_\odot$ compact objects, we need to estimate the primary stars' masses and inclination angles of the binary stars. As an illustration, let us consider a spectroscopic binary characterized by $\hat{f}_{m,\text{spectro}} = 1 M_\odot$ and inclination angle $i = 60^\circ$ (from which we obtain $f_{m,\text{spectro}} = 1.54 M_\odot$). If the primary star's mass is $1.2 M_\odot$, the secondary star's mass is $3 M_\odot$. In this case, the $3 M_\odot$ secondary star is highly likely a BH. In contrast, if the primary star's mass is $0.2 M_\odot$, the secondary star's mass is $1.9 M_\odot$. In this case, we cannot exclude the possibility that the $1.9 M_\odot$ secondary star is a main-sequence star outshined by the primary RGB star. From this simple illustrative example, we can see that the mass estimation of primary stars critically affects whether their secondary stars are BH or not.

Fortunately, these types of problems do not happen in our BH binary candidate. We know the inclination angle i of the binary star from the astrometric data, and get $f_{m,\text{spectro}}$ in a model-independent way. Moreover, this BH binary candidate has $f_{m,\text{astro}} > 5.68 M_\odot$ and $f_{m,\text{spectro}} > 6.75 M_\odot$ at a probability of 99 %. The secondary mass is more than $5 M_\odot$, even if this BH binary candidate is an Algol-type system, or the primary RGB mass is close to zero. The primary RGB star cannot outshine the $> 5 M_\odot$ secondary star even if the secondary star is in the main-sequence phase, or the faintest among $5 M_\odot$ stars in any phases except a BH. This point is described in detail below. Thus, the secondary star is likely to be a BH.

We examine the possibility that the secondary star of the BH binary candidate may be a single object except a BH, or multiple star systems. When a stellar mass is fixed, a MS star is the faintest except stellar remnants like WD, NS, and BH. If a MS star with the same mass as the secondary star is more luminous than the primary star, the possibility that the secondary star is a single object except a BH can be ruled out. When the total mass of a multiple star system is fixed, a multiple star system with equal-mass MS stars is the least luminous. This is because MS stars become luminous more steeply with their masses increasing. If an n -tuple star system with equal-mass MS stars has the same mass as

the secondary star, and larger luminosity than the primary star, the possibility that the secondary star is any n -tuple star systems can be rejected. Thus, we compare the luminosity of the primary star with the luminosities of a single MS star or multiple MS star systems with equal masses.

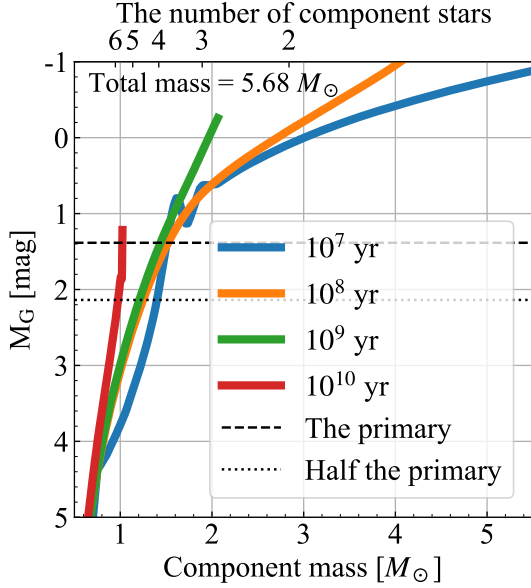


Figure 4. G-band absolute magnitude of multiple star systems with equal-mass MS stars whose ages are 10^7 , 10^8 , 10^9 , and 10^{10} yrs. The total mass of the multiple star systems is $5.68 M_{\odot}$, the lower bound mass of the secondary star of the BH binary candidate at a probability of 99 %. The component mass and the number of stars are shown in the lower and upper x -axis, respectively. We show only MS stars defined in Eq. (8). That is the reason why the curves of 10^9 and 10^{10} yrs cut off in the middle. We obtain G-band absolute magnitude and BP-RP color at each mass and age, using the PARSEC code (Bressan et al. 2012). The metallicity is set to the solar metallicity, the same as the primary star of the BH binary candidate. It seems that there is no publicly available spectroscopic survey data that provides reliable metallicity for the primary star of our BH binary candidate. The dashed line indicates the G-band absolute magnitude of the primary star, which is corrected by the G-band extinction. The dotted line indicates the G-band absolute magnitude of a star half as luminous as the primary star.

Figure 4 shows the G-band absolute magnitude of multiple star systems with equal-mass MS stars. The total mass of the multiple star systems is $5.68 M_{\odot}$, the lower bound mass of the secondary star of the BH binary candidate at a probability of 99 %. We can rule out single, binary and triple stars with the total mass of $5.68 M_{\odot}$. They would outshine the primary star if they were the secondary star. A quadruple star system with each stellar mass of 1.4 – $1.5 M_{\odot}$ is as luminous as the primary

star. However, such a quadruple star system should be detected by *Gaia* itself. A quintuple star system with each stellar mass of $1.1 M_{\odot}$ has luminosity twice less than the primary star, and might not be observed by *Gaia*. Except for multiple star systems with MS stars, the secondary star can be a triple NS star system or a quadruple WD star system, where the maximum mass of NS and WD are about 2.0 and $1.4 M_{\odot}$, respectively. Such systems may be more valuable than a single BH, since they have never been discovered to our knowledge. In any case, the secondary star should be quadruple or higher-order star systems except for a single BH. Moreover, the size of the system should be more compact than the pericenter distance of the primary star, ~ 2.4 au. It is unclear that such multiple systems are stable under the perturbation of the primary star.

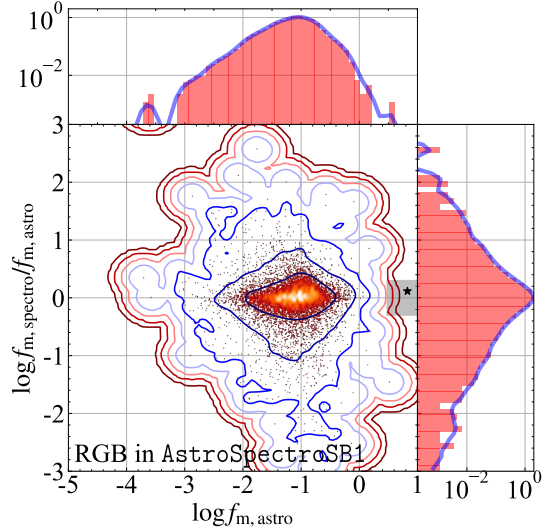


Figure 5. Bottom left: Scatter plots of $f_{m,astro}$ and $f_{m,spectro}/f_{m,astro}$ for RGB stars in *AstroSpectroSB1*. The color scale represents the square root of the relative density of binary stars. Contours indicate σ levels of 1, 2, \dots , and 7 from the inner to the outer. The shaded region is considered to calculate the p-values in Table 2. The p-values are calculated by a kernel-density estimate with the kernel bandwidth of Scott's rule (Scott 1992). The star point indicates the BH candidate (GDR3 source ID 5870569352746779008). It is not included in the samples with which the p-values are calculated. Top and left: $f_{m,astro}$ and $f_{m,spectro}/f_{m,astro}$ distributions, respectively. The histograms indicate the sample distribution, and the curves indicate the projected distributions derived by the kernel-density estimate.

In order to assess whether the BH binary candidate is coincidentally located on the $f_{m,astro} - f_{m,astro}/f_{m,spectro}$ plane, we calculate the p-values of a $f_{m,astro} - f_{m,astro}/f_{m,spectro}$ region around the BH binary candidate. We adopt a kernel-density estimate with

a kernel bandwidth of Scott’s rule (Scott 1992). The bandwidth is $N_{\text{sample}}^{-1/6}$, where N_{sample} is the number of samples. At first, we select RGB primary stars from *AstroSpectroSB1* as samples for the kernel-density estimate. The number of samples is 9047. Note that the BH binary candidate is excluded from the samples. Figure 5 shows the kernel-density contours of 1, 2, \dots , and 7σ levels from the inner to the outer. We calculate the p-value in the shaded region. The p-value is 9.6×10^{-12} , and the σ level is 6.1. The position of $f_{\text{m,astro}}$ and $f_{\text{m,astro}}/f_{\text{m,spectro}}$ of the BH binary candidate is unlikely to be coincident.

We select samples for the kernel-density estimate in different ways in order to investigate whether the p-values depend on the choice of samples. We summarize the choices of samples and their results in Table 2. The first column indicates the choice of samples. Note that the BH binary candidate is not included in any choices. For “All”, we choose all the samples selected in section 2. For “All in *AstroSpectroSB1*”, we choose all the samples in *AstroSpectroSB1*. For “RGBs in *AstroSpectroSB1*”, we extract only the RGB primary stars in the samples of “All in *AstroSpectroSB1*”. This is the samples shown in Figure 5. We also make samples, excluding samples with large errors of $f_{\text{m,astro}}$ and $f_{\text{m,spectro}}$ from “All in *AstroSpectroSB1*” and “RGBs in *AstroSpectroSB1*”. We calculate the errors in the same way as the one standard deviation of the BH binary candidate in Table 1, where we generate 10^3 Monte Carlo random draws for each sample for calculation cost savings. We adopt two cases to exclude samples. In the first case, we exclude 10 % samples with largest errors in either of $f_{\text{m,astro}}$ and $f_{\text{m,spectro}}$. In the second case, we exclude samples with errors larger than 0.2 in log-scale for either of $f_{\text{m,astro}}$ and $f_{\text{m,spectro}}$. Note that 0.2 is similar to the bandwidth of the kernel-density estimate. In any cases, the p-values are small, and the σ levels are high. The position of $f_{\text{m,astro}}$ and $f_{\text{m,astro}}/f_{\text{m,spectro}}$ of the BH binary candidate is unlikely to be coincident, independently of the choices of samples for the kernel-density estimate.

We search for the BH binary candidate in several database. The GDR3 variability table (Eyer et al. 2022) and the All-Sky Automated Survey for Supernovae (ASAS-SN; Kochanek et al. 2017) do not include the BH binary candidate as a variable star. Its light curve is available on the ASAS-SN Photometry

Database (Shappee et al. 2014; Jayasinghe et al. 2019)⁴ the BH binary candidate is not listed in the following data base: SIMBAD⁸, the ninth catalog of spectroscopic binary orbits (SB9; Pourbaix et al. 2004), RAdial Velocity Experiments (RAVE; Kunder et al. 2017), the Galactic Archaeology with HERMES (GALAH; Buder et al. 2021), the Large sky Area Multi-Object fiber Spectroscopic Surveys (LAMOST; Cui et al. 2012), and the Apache Point Observatory Galactic Evolution Experiment (APOGEE; Majewski et al. 2017). High-energy telescopes, such as the Fermi gamma-ray space telescope (Atwood et al. 2009), the Swift Burst Alert Telescope (Swift BAT; Barthelmy et al. 2005) XMM-Newton (Strüder et al. 2001), the Chandra observatory (Weiskopf et al. 2000), and the Galaxy Evolution Explorer (GALEX; Martin et al. 2005), do not observe it as far as we see Aladin lite⁹. ESO archive¹⁰ does not list it. In summary, we do not find any positive nor negative evidence for the BH binary candidate.

4. DISCUSSION

First, we compare the BH binary candidate with other BH binary candidates by previous studies, and assess whether our BH binary candidate is similar to others rejected before. As described in section 3, BH binary candidates tend to be rejected when their primary stars are RGB stars. It is difficult to estimate the masses of RGB stars, and such binary stars can be Algol-type systems in which primary stars are low-mass (say $\sim 0.1 M_{\odot}$). Since such BH binary candidates have $\hat{f}_{\text{m,spectro}} \sim 1 M_{\odot}$, the mass estimate of RGB stars severely affect the secondary mass. However, our BH binary candidate has $f_{\text{m,astro}} > 5.68 M_{\odot}$ and $f_{\text{m,spectro}} > 6.75 M_{\odot}$ at a probability of 99 %. In this case, the secondary mass is more than $\sim 5 M_{\odot}$ even if the primary mass is nearly zero. Note that the secondary mass increases monotonically with the primary mass increasing when $f_{\text{m,astro}}$ or $f_{\text{m,spectro}}$ is fixed. Thus, the secondary star is likely to

⁴ <https://asas-sn.osu.edu/photometry>. The BH binary candidate is observed in V and g band over ~ 3000 days. We do not find any periodic feature. The Transiting Exoplanet Survey Satellite (TESS; Ricker et al. 2015) has performed twice high-cadence observations during about 30 days according to data downloaded from TESScut⁵ for the BH binary candidate. The duration is too short to detect its periodic variability due to its binary orbit if any, since it has a period of about 1000 days. Wide-field Infrared Survey Explorer (WISE; Wright et al. 2010) also observes the BH binary candidate over ~ 4000 days according to ALLWISE Multiepoch Photometry Table⁶ and NEOWISE-R Single Exposure (L1b) Source Table⁷. We do not recognize any periodic variability. At the time of September 2022,

⁸ <http://simbad.cds.unistra.fr/simbad/>

⁹ <https://aladin.u-strasbg.fr/AladinLite/>

¹⁰ <http://archive.eso.org/scienceportal/home>

Table 2. P-values.

Sample	Number	p-value	σ level	Remark
All	64095	2.4×10^{-12}	7.0	
All in <i>AstroSpectroSB1</i>	33466	9.1×10^{-12}	6.8	
Low-error in <i>AstroSpectroSB1</i>	28188	1.0×10^{-11}	6.8	Exclude samples with top 10 % large errors
Low-error in <i>AstroSpectroSB1</i>	17614	1.1×10^{-11}	6.8	Exclude samples with errors more than 0.2 in log-scale
RGBs in <i>AstroSpectroSB1</i>	9047	9.6×10^{-12}	6.1	The same samples used in Figure 5
Low-error RGBs in <i>AstroSpectroSB1</i>	8626	7.5×10^{-10}	6.2	Exclude samples with top 10 % large errors
Low-error RGBs in <i>AstroSpectroSB1</i>	5395	1.2×10^{-9}	6.1	Exclude samples with errors more than 0.2 in log-scale

be a BH, even if the BH binary candidate is an Algol-type system.

[Gaia Collaboration et al. \(2022b\)](#) listed up BH binary candidates with $\sim 2 M_{\odot}$ MS stars and $\sim 3 M_{\odot}$ BHs. However, [El-Badry & Rix \(2022\)](#) pointed out possibility that they are Algol-type systems consisting of $\sim 0.2 M_{\odot}$ stripped stars and $\sim 2 M_{\odot}$ MS stars. The reason for this discrepancy is as follows. [Gaia Collaboration et al. \(2022b\)](#) thought that $\sim 2 M_{\odot}$ MS stars dominate the luminosity (photometry) and radial-velocity motion (spectroscopy) of the binary stars. On the other hand, [El-Badry & Rix \(2022\)](#) claimed that $\sim 2 M_{\odot}$ MS stars dominate the luminosity, while $\sim 0.2 M_{\odot}$ stripped stars dominate the radial-velocity motion. This interpretation better explains their spectral energy distribution and spectroscopic mass function ($\hat{f}_{m,\text{spectro}} \sim 1.5 M_{\odot}$) more naturally. We do not expect that similar things happen in our BH binary candidate for the following reason. If a hidden star dominates the radial-velocity motion, we replace m_2 with m_1 in Eq. (3). Since $f_{m,\text{astro}} \sim f_{m,\text{spectro}}$, we obtain $m_1 = 4f_{m,\text{astro}}(1 + F_2/F_1)^2 M_{\odot}$ and $m_2 = 4f_{m,\text{astro}}(1 + F_2/F_1)^2(1 + 2F_2/F_1) M_{\odot}$. Thus, the RGB primary mass should be at least $4f_{m,\text{astro}} (\sim 23) M_{\odot}$. However, its luminosity requires its mass much less than $23 M_{\odot}$. Thus, a hidden star does not dominate the radial-velocity motion of our BH binary candidate in contrary to the BH binary candidates in table 10 of [Gaia Collaboration et al. \(2022b\)](#).

[Gaia Collaboration et al. \(2022b\)](#) also show another table of BH binary candidates (their table 9) in which BH binary candidates belong to SB1, and have high $\hat{f}_{m,\text{spectro}} (> 3 M_{\odot})$. Hereafter, we call them ‘‘Gaia’s table 9 candidates’’. Although these candidates have secondary stars with more than $3 M_{\odot}$ for any primary masses, [Gaia Collaboration et al. \(2022b\)](#) cannot rule out that the secondary stars consist of multiple star systems, similarly to our description in section 3. We remark that our BH candidate will be better-constrained than all of Gaia’s

table 9 candidates. Our BH binary candidate has larger mass function and smaller luminosity than Gaia’s table 9 candidates except for GDR3 source IDs 4661290764764683776 and 5863544023161862144. GDR3 source ID 4661290764764683776 has high $\hat{f}_{m,\text{spectro}} (= 13.67 M_{\odot})$, however its primary star has high luminosity, -6.707 mag in G band. Since the primary star can be more luminous than a $\sim 13 M_{\odot}$ MS star, it is difficult to confirm that the secondary star is a BH. GDR3 source ID 5863544023161862144 shows eclipses, and consequently its secondary should not be a BH ([Gaia Collaboration et al. 2022b](#)). In summary, we can easiest rule out the possibility that the secondary star of our BH candidate consists of a multiple star system.

[Pourbaix et al. \(2022\)](#) and [Jayasinghe et al. \(2022a\)](#) compared orbital parameters in GDR3 with those in SB9 ([Pourbaix et al. 2004](#)), in particular for spectroscopic binary stars with either one component being parameterized (SB1). They found that Gaia’s and SB9’s periods are inconsistent for periods of more than 10^3 days in SB9. Since they did not investigate *AstroSpectroSB1*, we investigate both of SB1 and *AstroSpectroSB1*. We find 304 SB1 and 109 *AstroSpectroSB1* in common between GDR3 and SB9. Our BH binary candidate is not included in SB9 as described in the previous section. In Figure 6, we make comparison between orbital parameters of binary stars in GDR3 and SB9. Note that the x -axes in Figure 6 adopt GDR3 values, while [Pourbaix et al. \(2022\)](#) and [Jayasinghe et al. \(2022a\)](#) adopt SB9 values for the x -axes in their figure 7.41 and figure 6, respectively. Similarly to [Pourbaix et al. \(2022\)](#) and [Jayasinghe et al. \(2022a\)](#), we find that periods in GDR3 are largely different from those in SB9 for SB1 with periods of more than 10^3 days. However, for *AstroSpectroSB1*, their periods do not deviate up to periods of a few 10^3 days. The other parameters in GDR3 are also in good agreement with those in SB9 for *AstroSpectroSB1*, in particular around the mean values of the orbital param-

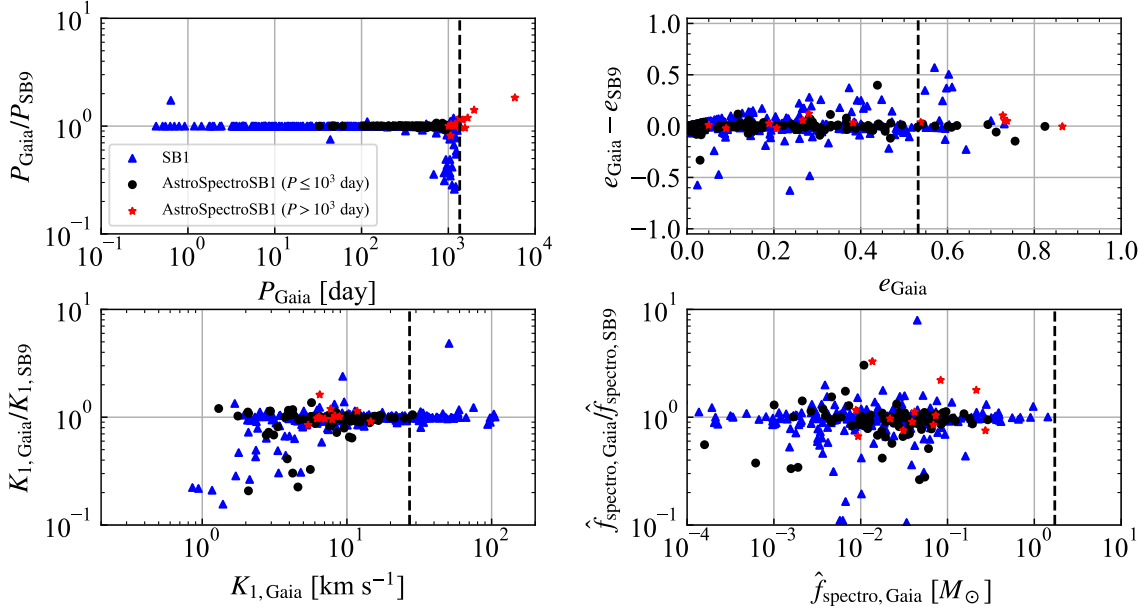


Figure 6. Comparison of orbital parameters (Period, eccentricity, radial velocity semi-amplitude, and $\hat{f}_{m,\text{spectro}}$) between GDR3 and SB9. Triangle, circle and star points indicate GDR3 SB1, AstroSpectroSB1 with a period of $\leq 10^3$ day, and AstroSpectroSB1 with a period of $> 10^3$ day, respectively. The dashed lines show the mean values of the orbital parameters of the BH binary candidate (GDR3 source ID 5870569352746779008).

eters of the BH binary candidate. This does not directly show that the spectroscopic data of the BH binary candidate is reliable, since most of binary stars in SB9 are brighter than our BH binary candidate. Nevertheless, this means that GDR3 values of AstroSpectroSB1 binary stars may be reliable even if the binary stars have periods of a few 10^3 days.

Bashi et al. (2022) compared GDR3 SB1 with the database of LAMOST (Cui et al. 2012) and GALAH (Buder et al. 2021), and found that GDR3 SB1 with periods of less than $10^{1.5}$ days may be refuted. Although our BH binary candidate belongs to AstroSpectroSB1 (not to SB1), it has a period of $\gtrsim 10^3$ days, much larger than $10^{1.5}$ days. Our BH binary candidate may not be refuted by the criteria of Bashi et al. (2022).

Andrews et al. (2022) and Shahaf et al. (2023) independently presented lists of NS and BH binary candidates in GDR3. Their lists do not include our BH binary candidate. This is because they focus on binary stars with primary MS stars. The masses of MS stars can be estimated less model-dependently than those of RGB stars. The masses and natures of secondary stars can be derived robustly. Thus, they avoided binary stars with primary RGB stars. On the other hand, although the primary star of our BH binary candidate is a RGB star, we can call it a “BH binary candidate”, because its $f_{m,\text{astro}}$ and $f_{m,\text{spectro}}$ are high; $\gtrsim 5.68$ and $6.75 M_\odot$, respectively, at a probability of 99 %. Its secondary mass is more than $5 M_\odot$, regardless of the primary RGB mass.

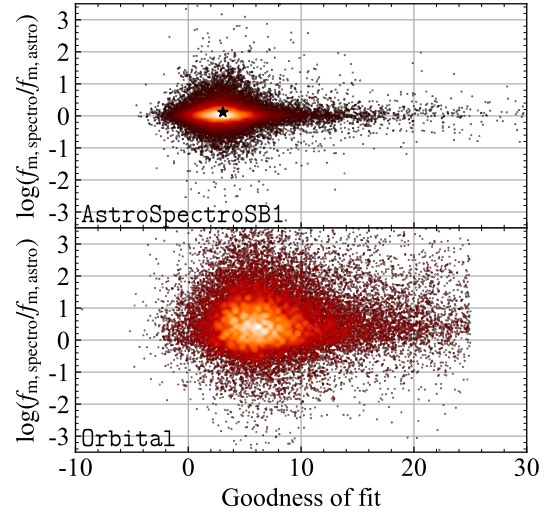


Figure 7. The ratio of $f_{m,\text{spectro}}$ to $f_{m,\text{astro}}$ as a function of goodness-of-fit values for AstroSpectroSB1 (top) and Orbital (bottom) binary stars. The color scale represents the square root of the relative density of binary stars. The star point indicates the BH binary candidate (GDR3 source ID 5870569352746779008).

Conversely, we examine the lists of Andrews et al. (2022) and Shahaf et al. (2023) from our conditions. We focus on binary stars with $m_2 > 2 M_\odot$ in their lists. Note that the maximum NS mass can be $\sim 2 M_\odot$. Our sample selected in section 2 does not include BH binary candidate in the Andrews’s list. The candidates

do not have spectroscopic data. This may be partly because astrometric binary stars with spectroscopic data (i.e. our sample) has systematically large goodness-of-fit values. Figure 7 shows that goodness-of-fit values in *AstroSpectroSB1* and *Orbital* are centered at ~ 3 and ~ 5 , respectively. Actually, this can be seen in the middle panel of figure 4 in Andrews et al. (2022). Their figure 4 includes all the *Orbital* binary stars with and without spectroscopic data, and indicates the second peak around the goodness-of-fit value of ~ 5 . The second peak should consist of *Orbital* binary stars with spectroscopic data. We do not know the reason for the systematic upward shift. We have to remark that bright binary stars (G band magnitude of < 13), i.e. those with spectroscopic data, have the systematically higher goodness-of-fit values, while faint binary stars (G band magnitude of > 13) typically have lower goodness-of-fit values¹¹. In any case, our sample does not include the list of Andrews et al. (2022), because they avoid including binary stars with goodness-of-fit values of more than 5 in their list.

Our sample includes Shanaf’s three BH binary candidates (GDR3 source IDs: 3263804373319076480, 3509370326763016704, and 6281177228434199296). However, we do not list up them as BH binary candidates. This is because their $f_{m,spectro}/f_{m,astro}$ are small (0.25, 0.0053, 0.0017, respectively) for our first condition as seen in Eq. (6). We do not intend to reject the three BH candidates completely. The three BH candidates may suffer from large errors of spectroscopic data, and consequently have small $f_{m,spectro}/f_{m,astro}$. We suspect this possibility, because two of the three BH candidates are not included in *AstroSpectroSB1* binary stars despite the fact that they have spectroscopic data. Our sample selected in section 2 does not include the other 5 BH binary candidates because of the absence of spectroscopic data.

A few days after we posted this work on arXiv, El-Badry et al. (2023a) reported one promising BH binary candidate different from our BH binary candidate. They made follow-up spectroscopic observation, and showed that *Gaia*’s astrometric data is consistent with their spectroscopic data. Since their BH binary candidate has a shorter period (185.6 days) than our binary candidate (1352.22 days), they can finish their follow-up observation in a short period of time. They also mentioned our BH binary candidate, and did not conclude whether our BH binary candidate is genuine because of the absence of follow-up spectroscopic observations. Their argument

is in good agreement with ours. Note that we analyze our BH binary candidate in detail.

Several BH binary candidates can be rejected for exceptional reasons. Although *Gaia Collaboration et al. (2022b)* found that GDR3 source ID 2006840790676091776 has high $\hat{f}_{m,spectro}$, they did not include it in their list of BH binary candidates. This is because it is close to a bright star, whose apparent magnitude is 3.86 mag in G band. There is no such bright stars close to our BH binary candidate. Nearby stars have apparent magnitude of at least 13 mag in G band. The reason for this rejection can not be applied to our BH binary candidate. Andrews et al. (2022) removed GDR3 source ID 4373465352415301632¹², since its period (~ 186 days) is roughly 3 times *Gaia*’s scanning period (63 days). Our BH binary candidate has a period of 1352 days, not integer multiple of *Gaia*’s scanning period.

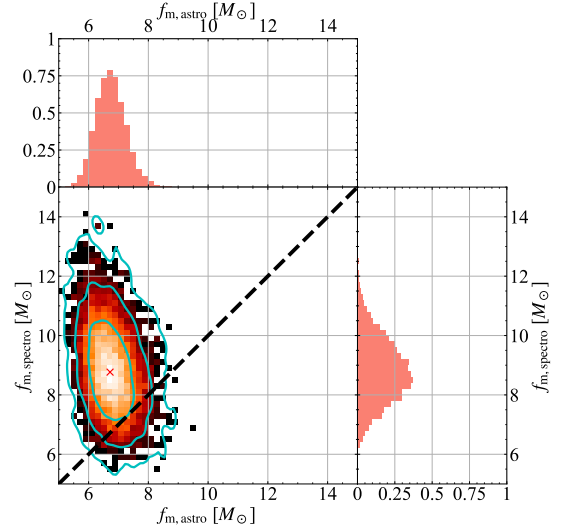


Figure 8. Bottom left: 2-dimensional probability distribution of $f_{m,astro}$ and $f_{m,spectro}$ for the BH binary candidate (GDR3 source ID 5870569352746779008). The cross point means the typical values of $f_{m,astro}$ and $f_{m,spectro}$. Contours indicate σ levels of 1, 2, and 3 from the inner to the outer. The dashed line shows $f_{m,astro} = f_{m,spectro}$. Top and left: $f_{m,astro}$ and $f_{m,spectro}$ distributions, respectively.

Hereafter, we make several concerns. First of all, we mostly rely on GDR3 astrometric and spectroscopic data, which are already largely processed. We do not assess correctness of the data of our BH binary candidate. Aside from this, we find that the BH binary candidate has $f_{m,spectro} > f_{m,astro}$ and $f_{m,spectro} < f_{m,astro}$ at

¹¹ The exact value of 13 is obtained by El-Badry et al. (2023b).

¹² This object is later confirmed as a BH binary (also known as Gaia BH1) by El-Badry et al. (2023a).

probabilities of 95 and 5 %, respectively (see Table 1). Although $f_{m,\text{spectro}} = f_{m,\text{astro}}$ is possible, $f_{m,\text{spectro}}$ is always larger than $f_{m,\text{astro}}$ in the 1σ -level region as seen in Figure 8. For comparison, we calculate the probabilities of $f_{m,\text{spectro}} > f_{m,\text{astro}}$ and $f_{m,\text{spectro}} < f_{m,\text{astro}}$ for GDR3 source ID 5136025521527939072 which is in `AstroSpectroSB1`, and suggested as a NS binary candidate by Gaia Collaboration et al. (2022b)¹³. They are 72 and 28 %. Both of $f_{m,\text{spectro}} > f_{m,\text{astro}}$ and $f_{m,\text{spectro}} < f_{m,\text{astro}}$ are in the 1σ -level region, in contrast to our BH binary candidate. The $f_{m,\text{spectro}}$ and $f_{m,\text{astro}}$ of our BH binary candidate are not as similar as those of GDR3 source ID 5136025521527939072. Nevertheless, we may regard $f_{m,\text{spectro}} = f_{m,\text{astro}}$, since our BH binary candidate may contain some systematic error in either of spectroscopic or astrometric data.

Another concern is that the primary star of the BH binary candidate is a RGB star. Theoretical studies (e.g. Shikauchi et al. 2020, 2022) expected that a BH binary with a $\gtrsim 10 M_{\odot}$ MS primary star is likely to be found first (but see also Shikauchi et al. 2023). This is because such MS stars are bright, and can be observed even if they are distant. Moreover, they are longer-lived than RGB stars with similar masses. However, GDR3 does not present orbital parameters of binary stars with $\gtrsim 10 M_{\odot}$ MS primary stars in `AstroSpectroSB1` nor `Orbital` according to the GDR3 `binary_masses` table obtained with the ADQL query in section 2.2. We do not know the reason for the absence of such binary stars in GDR3. Nevertheless, when there are no such binary stars, it may be natural that a BH binary with a RGB star is first discovered.

We need two types of follow-up observations in order to assess if the BH binary candidate is true or not. The first type should be spectroscopic observations to verify the GDR3 spectroscopic data, and to perform spectral disentangling of the BH binary candidate similar to El-Badry & Rix (2022). The second type should be deep photometric observations. Such observations could constrain whether the secondary star is a BH, or consists of multiple stars. We remark that El-Badry et al. (2023b) have carried out these follow-up observations, and confirmed it as a genuine BH binary, Gaia BH2. This demonstrates that these follow-up observations would be important for confirming or refuting future BH candidates, which may be discovered by our search methodology in upcoming Gaia data.

5. SUMMARY

We first search for BH binary candidates from astrometric binary stars with spectroscopic data in GDR3. From the sample of 64108 binary stars, we find one BH binary candidate. The GDR3 source ID is 5870569352746779008. Since its primary star is a RGB star, we cannot estimate the mass of the primary RGB star. However, because of its high astrometric and spectroscopic mass function ($f_{m,\text{astro}} > 5.68 M_{\odot}$ and $f_{m,\text{spectro}} > 6.75 M_{\odot}$ at a probability of 99 %), the secondary star should have more than $5 M_{\odot}$, and is likely to be a BH, regardless of the primary mass. Unless the secondary star is a BH, it must be quadruple or higher-order multiple star systems with the total mass of $5.68 M_{\odot}$. To rule out the possibility of multiple star systems, we need deep photometric observations. Rather, if it is quadruple or higher-order multiple star systems, long-term observation may find modulation of the primary's orbit (e.g. Hayashi et al. 2020; Hayashi & Suto 2020; Liu et al. 2022).

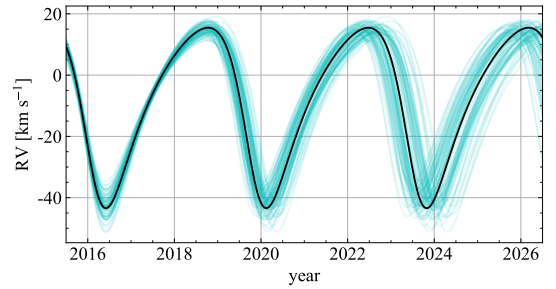


Figure 9. Predicted radial velocities of the BH binary candidate (GDR3 source ID 5136025521527939072), based on GDR3. The black curve can be obtained from typical values in GDR3. We generate cyan curves from 10^2 Monte Carlo random draws, using the covariance matrix. The radial velocity amplitude is larger and the turnover time spreads more widely than those in the upper panel of figure 3 in (El-Badry et al. 2023b), because we do not adopt any explicit link between the spectroscopic and astrometric Thiele-Innes parameters.

The weakness of this paper is that our conclusion entirely relies on the Gaia DR3. In particular, our BH binary candidate has a period of ~ 1300 days, more than a period of 34 months of the Gaia DR3 data collection. Our conclusion have to be confirmed by follow-up observations. For example, we need the time evolution of the radial velocity of our BH binary candidate similarly to that of Gaia BH1 obtained by El-Badry et al. (2023a). Figure 9 shows the predicted radial velocities of the BH binary candidate. Eventually, El-Badry et al. (2023b) have confirmed the radial velocity variability, by observing it ~ 30 times from the last half of 2022

¹³ The NS binary candidate is more likely to be a WD binary according to El-Badry et al. (2023a).

to the beginning of 2023, when the radial velocities had steeply decreased.

Previously, RGB stars harboring BHs have not been searched for because of the difficulty of the mass estimation of the RGB stars (and thus BHs). However, our tentative discovery in this paper encourages us to explore not only BHs orbiting around MS stars but also BHs orbiting around RGB stars in the future data releases of *Gaia*.

ACKNOWLEDGMENTS

We thank the anonymous referee for many fruitful advices. This research could not been accomplished without the support by Grants-in-Aid for Scientific Research (17H06360, 19K03907) from the Japan Society for the Promotion of Science. KH is supported by JSPS KAKENHI Grant Numbers JP21K13965 and JP21H00053. NK is supported by JSPS KAKENHI Grant Numbers JP22K03686. TK is supported by JSPD KAKENHI Grant Number JP21K13915, and JP22K03630. MS ac-

knowledges support by Research Fellowships of Japan Society for the Promotion of Science for Young Scientists, by Forefront Physics and Mathematics Program to Drive Transformation (FoPM), a World-leading Innovative Graduate Study (WINGS) Program, the University of Tokyo, and by JSPS Overseas Challenge Program for Young Researchers.

This work presents results from the European Space Agency (ESA) space mission *Gaia*. *Gaia* data are being processed by the *Gaia* Data Processing and Analysis Consortium (DPAC). Funding for the DPAC is provided by national institutions, in particular the institutions participating in the *Gaia* MultiLateral Agreement (MLA). The *Gaia* mission website is <https://www.cosmos.esa.int/gaia>. The *Gaia* archive website is <https://archives.esac.esa.int/gaia>.

Software: Matplotlib (Hunter 2007); NumPy (van der Walt et al. 2011); Astropy (Astropy Collaboration et al. 2013); SciPy (Virtanen et al. 2020)

REFERENCES

- Abbott, B. P., Abbott, R., Abbott, T. D., et al. 2019, *Physical Review X*, 9, 031040, doi: [10.1103/PhysRevX.9.031040](https://doi.org/10.1103/PhysRevX.9.031040)
- Abbott, R., Abbott, T. D., Abraham, S., et al. 2021, *Physical Review X*, 11, 021053, doi: [10.1103/PhysRevX.11.021053](https://doi.org/10.1103/PhysRevX.11.021053)
- Abdul-Masih, M., Banyard, G., Bodensteiner, J., et al. 2020, *Nature*, 580, E11, doi: [10.1038/s41586-020-2216-x](https://doi.org/10.1038/s41586-020-2216-x)
- Andrews, J. J. 2022, arXiv e-prints, arXiv:2206.04648. <https://arxiv.org/abs/2206.04648>
- Andrews, J. J., Breivik, K., & Chatterjee, S. 2019, *ApJ*, 886, 68, doi: [10.3847/1538-4357/ab441f](https://doi.org/10.3847/1538-4357/ab441f)
- Andrews, J. J., Breivik, K., Chawla, C., Rodriguez, C., & Chatterjee, S. 2021, arXiv e-prints, arXiv:2110.05549. <https://arxiv.org/abs/2110.05549>
- Andrews, J. J., Taggart, K., & Foley, R. 2022, arXiv e-prints, arXiv:2207.00680. <https://arxiv.org/abs/2207.00680>
- Astropy Collaboration, Robitaille, T. P., Tollerud, E. J., et al. 2013, *A&A*, 558, A33, doi: [10.1051/0004-6361/201322068](https://doi.org/10.1051/0004-6361/201322068)
- Atwood, W. B., Abdo, A. A., Ackermann, M., et al. 2009, *ApJ*, 697, 1071, doi: [10.1088/0004-637X/697/2/1071](https://doi.org/10.1088/0004-637X/697/2/1071)
- Barthelmy, S. D., Barbier, L. M., Cummings, J. R., et al. 2005, *SSRv*, 120, 143, doi: [10.1007/s11214-005-5096-3](https://doi.org/10.1007/s11214-005-5096-3)
- Bashi, D., Shahaf, S., Mazeh, T., et al. 2022, *MNRAS*, 517, 3888, doi: [10.1093/mnras/stac2928](https://doi.org/10.1093/mnras/stac2928)
- Binnendijk, L. 1960, Properties of double stars; a survey of parallaxes and orbits.
- Bodensteiner, J., Shenar, T., Mahy, L., et al. 2020, *A&A*, 641, A43, doi: [10.1051/0004-6361/202038682](https://doi.org/10.1051/0004-6361/202038682)
- Breivik, K., Chatterjee, S., & Larson, S. L. 2017, *ApJL*, 850, L13, doi: [10.3847/2041-8213/aa97d5](https://doi.org/10.3847/2041-8213/aa97d5)
- Bressan, A., Marigo, P., Girardi, L., et al. 2012, *MNRAS*, 427, 127, doi: [10.1111/j.1365-2966.2012.21948.x](https://doi.org/10.1111/j.1365-2966.2012.21948.x)
- Buder, S., Sharma, S., Kos, J., et al. 2021, *MNRAS*, 506, 150, doi: [10.1093/mnras/stab1242](https://doi.org/10.1093/mnras/stab1242)
- Casares, J., Jonker, P. G., & Israelian, G. 2017, *X-Ray Binaries*, ed. A. W. Alsabti & P. Murdin, 1499, doi: [10.1007/978-3-319-21846-5_111](https://doi.org/10.1007/978-3-319-21846-5_111)
- Chakrabarti, S., Simon, J. D., Craig, P. A., et al. 2022, arXiv e-prints, arXiv:2210.05003. <https://arxiv.org/abs/2210.05003>
- Chawla, C., Chatterjee, S., Breivik, K., et al. 2022, *ApJ*, 931, 107, doi: [10.3847/1538-4357/ac60a5](https://doi.org/10.3847/1538-4357/ac60a5)
- Corral-Santana, J. M., Casares, J., Muñoz-Darias, T., et al. 2016, *A&A*, 587, A61, doi: [10.1051/0004-6361/201527130](https://doi.org/10.1051/0004-6361/201527130)
- Cui, X.-Q., Zhao, Y.-H., Chu, Y.-Q., et al. 2012, *Research in Astronomy and Astrophysics*, 12, 1197, doi: [10.1088/1674-4527/12/9/003](https://doi.org/10.1088/1674-4527/12/9/003)
- El-Badry, K., & Burdge, K. B. 2022, *MNRAS*, 511, 24, doi: [10.1093/mnras/rlab135](https://doi.org/10.1093/mnras/rlab135)
- El-Badry, K., Burdge, K. B., & Mróz, P. 2022a, *MNRAS*, 511, 3089, doi: [10.1093/mnras/stac274](https://doi.org/10.1093/mnras/stac274)

- El-Badry, K., & Quataert, E. 2020, MNRAS, 493, L22, doi: [10.1093/mnras/slaa004](https://doi.org/10.1093/mnras/slaa004)
- . 2021, MNRAS, 502, 3436, doi: [10.1093/mnras/stab285](https://doi.org/10.1093/mnras/stab285)
- El-Badry, K., & Rix, H.-W. 2022, MNRAS, 515, 1266, doi: [10.1093/mnras/stac1797](https://doi.org/10.1093/mnras/stac1797)
- El-Badry, K., Seeburger, R., Jayasinghe, T., et al. 2022b, MNRAS, 512, 5620, doi: [10.1093/mnras/stac815](https://doi.org/10.1093/mnras/stac815)
- El-Badry, K., Rix, H.-W., Quataert, E., et al. 2023a, MNRAS, 518, 1057, doi: [10.1093/mnras/stac3140](https://doi.org/10.1093/mnras/stac3140)
- El-Badry, K., Rix, H.-W., Cendes, Y., et al. 2023b, arXiv e-prints, arXiv:2302.07880. <https://arxiv.org/abs/2302.07880>
- Eldridge, J. J., Stanway, E. R., Breivik, K., et al. 2020, MNRAS, 495, 2786, doi: [10.1093/mnras/staa1324](https://doi.org/10.1093/mnras/staa1324)
- Eyer, L., Audard, M., Holl, B., et al. 2022, arXiv e-prints, arXiv:2206.06416. <https://arxiv.org/abs/2206.06416>
- Fu, J.-B., Gu, W.-M., Zhang, Z.-X., et al. 2022, ApJ, 940, 126, doi: [10.3847/1538-4357/ac9b4c](https://doi.org/10.3847/1538-4357/ac9b4c)
- Gaia Collaboration, Prusti, T., de Bruijne, J. H. J., et al. 2016, A&A, 595, A1, doi: [10.1051/0004-6361/201629272](https://doi.org/10.1051/0004-6361/201629272)
- Gaia Collaboration, Brown, A. G. A., Vallenari, A., et al. 2018a, A&A, 616, A1, doi: [10.1051/0004-6361/201833051](https://doi.org/10.1051/0004-6361/201833051)
- Gaia Collaboration, Babusiaux, C., van Leeuwen, F., et al. 2018b, A&A, 616, A10, doi: [10.1051/0004-6361/201832843](https://doi.org/10.1051/0004-6361/201832843)
- Gaia Collaboration, Brown, A. G. A., Vallenari, A., et al. 2021, A&A, 650, C3, doi: [10.1051/0004-6361/202039657e](https://doi.org/10.1051/0004-6361/202039657e)
- Gaia Collaboration, Vallenari, A., Brown, A. G. A., et al. 2022a, arXiv e-prints, arXiv:2208.00211. <https://arxiv.org/abs/2208.00211>
- Gaia Collaboration, Arenou, F., Babusiaux, C., et al. 2022b, arXiv e-prints, arXiv:2206.05595. <https://arxiv.org/abs/2206.05595>
- Giesers, B., Dreizler, S., Husser, T.-O., et al. 2018, MNRAS, 475, L15, doi: [10.1093/mnrasl/slx203](https://doi.org/10.1093/mnrasl/slx203)
- Gomel, R., Mazeh, T., Faigler, S., et al. 2022, arXiv e-prints, arXiv:2206.06032. <https://arxiv.org/abs/2206.06032>
- Halbwachs, J.-L., Pourbaix, D., Arenou, F., et al. 2022, arXiv e-prints, arXiv:2206.05726. <https://arxiv.org/abs/2206.05726>
- Hayashi, T., & Suto, Y. 2020, ApJ, 897, 29, doi: [10.3847/1538-4357/ab97ad](https://doi.org/10.3847/1538-4357/ab97ad)
- Hayashi, T., Wang, S., & Suto, Y. 2020, ApJ, 890, 112, doi: [10.3847/1538-4357/ab6de6](https://doi.org/10.3847/1538-4357/ab6de6)
- Heintz, W. D. 1978, Double stars, Vol. 15
- Holl, B., Sozzetti, A., Sahlmann, J., et al. 2022a, arXiv e-prints, arXiv:2206.05439. <https://arxiv.org/abs/2206.05439>
- Holl, B., Fabricius, C., Portell, J., et al. 2022b, arXiv e-prints, arXiv:2212.11971. <https://arxiv.org/abs/2212.11971>
- Hunter, J. D. 2007, Computing in Science and Engineering, 9, 90, doi: [10.1109/MCSE.2007.55](https://doi.org/10.1109/MCSE.2007.55)
- Irrgang, A., Geier, S., Kreuzer, S., Pelisoli, I., & Heber, U. 2020, A&A, 633, L5, doi: [10.1051/0004-6361/201937343](https://doi.org/10.1051/0004-6361/201937343)
- Janssens, S., Shenar, T., Sana, H., et al. 2022, A&A, 658, A129, doi: [10.1051/0004-6361/202141866](https://doi.org/10.1051/0004-6361/202141866)
- Jayasinghe, T., Rowan, D. M., Thompson, T. A., Kochanek, C. S., & Stanek, K. Z. 2022a, arXiv e-prints, arXiv:2207.05086. <https://arxiv.org/abs/2207.05086>
- Jayasinghe, T., Stanek, K. Z., Kochanek, C. S., et al. 2019, MNRAS, 485, 961, doi: [10.1093/mnras/stz444](https://doi.org/10.1093/mnras/stz444)
- Jayasinghe, T., Stanek, K. Z., Thompson, T. A., et al. 2021, MNRAS, 504, 2577, doi: [10.1093/mnras/stab907](https://doi.org/10.1093/mnras/stab907)
- Jayasinghe, T., Thompson, T. A., Kochanek, C. S., et al. 2022b, MNRAS, doi: [10.1093/mnras/stac2187](https://doi.org/10.1093/mnras/stac2187)
- Kalogera, V., & Baym, G. 1996, ApJL, 470, L61, doi: [10.1086/310296](https://doi.org/10.1086/310296)
- Kinugawa, T., & Yamaguchi, M. S. 2018, arXiv e-prints. <https://arxiv.org/abs/1810.09721>
- Kochanek, C. S., Shappee, B. J., Stanek, K. Z., et al. 2017, PASP, 129, 104502, doi: [10.1088/1538-3873/aa80d9](https://doi.org/10.1088/1538-3873/aa80d9)
- Kunder, A., Kordopatis, G., Steinmetz, M., et al. 2017, AJ, 153, 75, doi: [10.3847/1538-3881/153/2/75](https://doi.org/10.3847/1538-3881/153/2/75)
- Lallement, R., Vergely, J. L., Babusiaux, C., & Cox, N. L. J. 2022, A&A, 661, A147, doi: [10.1051/0004-6361/202142846](https://doi.org/10.1051/0004-6361/202142846)
- Lennon, D. J., Dufton, P. L., Villaseñor, J. I., et al. 2022, A&A, 665, A180, doi: [10.1051/0004-6361/202142413](https://doi.org/10.1051/0004-6361/202142413)
- Liu, B., D’Orazio, D. J., Vigna-Gómez, A., & Samsing, J. 2022, PhRvD, 106, 123010, doi: [10.1103/PhysRevD.106.123010](https://doi.org/10.1103/PhysRevD.106.123010)
- Liu, J., Zhang, H., Howard, A. W., et al. 2019, Nature, 575, 618, doi: [10.1038/s41586-019-1766-2](https://doi.org/10.1038/s41586-019-1766-2)
- Majewski, S. R., Schiavon, R. P., Frinchaboy, P. M., et al. 2017, AJ, 154, 94, doi: [10.3847/1538-3881/aa784d](https://doi.org/10.3847/1538-3881/aa784d)
- Martin, D. C., Fanson, J., Schiminovich, D., et al. 2005, ApJL, 619, L1, doi: [10.1086/426387](https://doi.org/10.1086/426387)
- Mashian, N., & Loeb, A. 2017, MNRAS, 470, 2611, doi: [10.1093/mnras/stx1410](https://doi.org/10.1093/mnras/stx1410)
- Pourbaix, D., Tokovinin, A. A., Batten, A. H., et al. 2004, A&A, 424, 727, doi: [10.1051/0004-6361:20041213](https://doi.org/10.1051/0004-6361:20041213)
- Pourbaix, D., Arenou, F., Gavras, P., et al. 2022, Gaia DR3 documentation Chapter 7: Non-single stars
- Ricker, G. R., Winn, J. N., Vanderspek, R., et al. 2015, Journal of Astronomical Telescopes, Instruments, and Systems, 1, 014003, doi: [10.1117/1.JATIS.1.1.014003](https://doi.org/10.1117/1.JATIS.1.1.014003)

- Rivinius, T., Baade, D., Hadrava, P., Heida, M., & Klement, R. 2020, *A&A*, 637, L3, doi: [10.1051/0004-6361/202038020](https://doi.org/10.1051/0004-6361/202038020)
- Safarzadeh, M., Ramirez-Ruiz, E., & Kilpatrick, C. 2020, *ApJ*, 901, 116, doi: [10.3847/1538-4357/abb0e8](https://doi.org/10.3847/1538-4357/abb0e8)
- Sana, H., de Mink, S. E., de Koter, A., et al. 2012, *Science*, 337, 444, doi: [10.1126/science.1223344](https://doi.org/10.1126/science.1223344)
- Saracino, S., Kamann, S., Guarcello, M. G., et al. 2022, *MNRAS*, 511, 2914, doi: [10.1093/mnras/stab3159](https://doi.org/10.1093/mnras/stab3159)
- Scott, D. W. 1992, *Multivariate Density Estimation*
- Shahaf, S., Bashi, D., Mazeh, T., et al. 2023, *MNRAS*, 518, 2991, doi: [10.1093/mnras/stac3290](https://doi.org/10.1093/mnras/stac3290)
- Shahaf, S., Mazeh, T., Faigler, S., & Holl, B. 2019, *MNRAS*, 487, 5610, doi: [10.1093/mnras/stz1636](https://doi.org/10.1093/mnras/stz1636)
- Shao, Y., & Li, X.-D. 2019, *ApJ*, 885, 151, doi: [10.3847/1538-4357/ab4816](https://doi.org/10.3847/1538-4357/ab4816)
- Shapiro, S. L., & Teukolsky, S. A. 1983, *Black holes, white dwarfs, and neutron stars : the physics of compact objects*
- Shappee, B. J., Prieto, J. L., Grupe, D., et al. 2014, *ApJ*, 788, 48, doi: [10.1088/0004-637X/788/1/48](https://doi.org/10.1088/0004-637X/788/1/48)
- Shenar, T., Bodensteiner, J., Abdul-Masih, M., et al. 2020, *A&A*, 639, L6, doi: [10.1051/0004-6361/202038275](https://doi.org/10.1051/0004-6361/202038275)
- Shenar, T., Sana, H., Mahy, L., et al. 2022, *Nature Astronomy*, 6, 1085, doi: [10.1038/s41550-022-01730-y](https://doi.org/10.1038/s41550-022-01730-y)
- Shikauchi, M., Kumamoto, J., Tanikawa, A., & Fujii, M. S. 2020, *PASJ*, 72, 45, doi: [10.1093/pasj/psaa030](https://doi.org/10.1093/pasj/psaa030)
- Shikauchi, M., Tanikawa, A., & Kawanaka, N. 2022, *ApJ*, 928, 13, doi: [10.3847/1538-4357/ac5329](https://doi.org/10.3847/1538-4357/ac5329)
- Shikauchi, M., Tsuna, D., Tanikawa, A., & Kawanaka, N. 2023, *arXiv e-prints*, arXiv:2301.07207, doi: [10.48550/arXiv.2301.07207](https://doi.org/10.48550/arXiv.2301.07207)
- Strüder, L., Briel, U., Dennerl, K., et al. 2001, *A&A*, 365, L18, doi: [10.1051/0004-6361:20000066](https://doi.org/10.1051/0004-6361:20000066)
- Tanikawa, A., Kinugawa, T., Kumamoto, J., & Fujii, M. S. 2020, *PASJ*, 72, 39, doi: [10.1093/pasj/psaa021](https://doi.org/10.1093/pasj/psaa021)
- The LIGO Scientific Collaboration, The Virgo Collaboration, & The KAGRA Scientific Collaboration. 2021, *arXiv e-prints*, arXiv:2111.03634, <https://arxiv.org/abs/2111.03634>
- Thompson, T. A., Kochanek, C. S., Stanek, K. Z., et al. 2019, *Science*, 366, 637, doi: [10.1126/science.aau4005](https://doi.org/10.1126/science.aau4005)
- van den Heuvel, E. P. J., Bhattacharya, D., Nomoto, K., & Rappaport, S. A. 1992, *A&A*, 262, 97
- van den Heuvel, E. P. J., & Tauris, T. M. 2020, *Science*, 368, eaba3282, doi: [10.1126/science.aba3282](https://doi.org/10.1126/science.aba3282)
- van der Walt, S., Colbert, S. C., & Varoquaux, G. 2011, *Computing in Science and Engineering*, 13, 22, doi: [10.1109/MCSE.2011.37](https://doi.org/10.1109/MCSE.2011.37)
- Vergely, J. L., Lallement, R., & Cox, N. L. J. 2022, *A&A*, 664, A174, doi: [10.1051/0004-6361/202243319](https://doi.org/10.1051/0004-6361/202243319)
- Virtanen, P., Gommers, R., Oliphant, T. E., et al. 2020, *Nature Methods*, 17, 261, doi: [10.1038/s41592-019-0686-2](https://doi.org/10.1038/s41592-019-0686-2)
- Weisskopf, M. C., Tananbaum, H. D., Van Speybroeck, L. P., & O'Dell, S. L. 2000, in *Society of Photo-Optical Instrumentation Engineers (SPIE) Conference Series*, Vol. 4012, *X-Ray Optics, Instruments, and Missions III*, ed. J. E. Truemper & B. Aschenbach, 2–16, doi: [10.1117/12.391545](https://doi.org/10.1117/12.391545)
- Woosley, S. E., Heger, A., & Weaver, T. A. 2002, *Reviews of Modern Physics*, 74, 1015, doi: [10.1103/RevModPhys.74.1015](https://doi.org/10.1103/RevModPhys.74.1015)
- Wright, E. L., Eisenhardt, P. R. M., Mainzer, A. K., et al. 2010, *AJ*, 140, 1868, doi: [10.1088/0004-6256/140/6/1868](https://doi.org/10.1088/0004-6256/140/6/1868)
- Yalinewich, A., Beniamini, P., Hotokezaka, K., & Zhu, W. 2018, *MNRAS*, 481, 930, doi: [10.1093/mnras/sty2327](https://doi.org/10.1093/mnras/sty2327)
- Yamaguchi, M. S., Kawanaka, N., Bulik, T., & Piran, T. 2018, *ApJ*, 861, 21, doi: [10.3847/1538-4357/aac5ec](https://doi.org/10.3847/1538-4357/aac5ec)